

## Free radical stress-mediated loss of *Kcnj10* protein expression in stria vascularis contributes to deafness in Pendred syndrome mouse model

Ruchira Singh and Philine Wangemann

Department of Anatomy and Physiology, Kansas State University, Manhattan, Kansas

Submitted 15 September 2007; accepted in final form 22 October 2007

**Singh R, Wangemann P.** Free radical stress-mediated loss of *Kcnj10* protein expression in stria vascularis contributes to deafness in Pendred syndrome mouse model. *Am J Physiol Renal Physiol* 294: F139–F148, 2008. First published October 24, 2007; doi:10.1152/ajprenal.00433.2007.—Pendred syndrome is due to loss-of-function mutations of *Slc26a4*, which codes for the HCO<sub>3</sub><sup>-</sup> transporter pendrin. Loss of pendrin causes deafness via a loss of the K<sup>+</sup> channel *Kcnj10* in stria vascularis and consequent loss of the endocochlear potential. Pendrin and *Kcnj10* are expressed in different cell types. Here, we report that free radical stress provides a link between the loss of *Kcnj10* and the loss of pendrin. Studies were performed using native and cultured stria vascularis from *Slc26a4*<sup>+/-</sup> and *Slc26a4*<sup>-/-</sup> mice as well as Chinese hamster ovary (CHO)-K1 cells. *Kcnj10*, oxidized proteins, and proteins involved in iron metabolism were quantified by Western blotting. Nitrated proteins were quantified by ELISA. Total iron was measured by ferrozine spectrophotometry and gene expression was quantified by qRT-PCR. At postnatal day 10 (P10), stria vascularis from *Slc26a4*<sup>+/-</sup> and *Slc26a4*<sup>-/-</sup> mice expressed similar amounts of *Kcnj10*. *Slc26a4*<sup>-/-</sup> mice lost *Kcnj10* expression during the next 5 days of development. In contrast, stria vascularis, obtained from P10 *Slc26a4*<sup>-/-</sup> mice and kept in culture for 5 days, maintained *Kcnj10* expression. Stria vascularis from *Slc26a4*<sup>-/-</sup> mice was found to suffer from free radical stress evident by elevated amounts of oxidized and nitrated proteins and other changes in protein and gene expression. Free radical stress induced by 3-morpholinopyridone-*N*-ethylcarbamide was found to be sufficient to reduce *Kcnj10* expression in CHO-K1 cells. These data demonstrate that free radical stress provides a link between loss of pendrin and loss of *Kcnj10* in *Slc26a4*<sup>-/-</sup> mice and possibly in human patients suffering from Pendred syndrome.

cochlea; pendrin; oxidation; nitration

PENDRED SYNDROME, THE MOST frequent hereditary form of syndromic deafness, is an autosomal recessive disease that affects the inner ear and the thyroid and causes childhood deafness and postpuberty goiter (9, 21, 29). It is caused by loss-of-function mutations of the gene *SLC26A4*, which encodes the anion exchanger pendrin (13, 16, 32). Pendrin has been characterized in heterologous expression systems to be an anion exchanger that accepts Cl<sup>-</sup>, HCO<sub>3</sub><sup>-</sup>, I<sup>-</sup>, and formate (37).

Investigations of the cause of deafness in Pendred syndrome have recently been facilitated by the creation of mouse model (12). The following observations have been made in the Pendred syndrome mouse model: 1) enlargement of endolymphatic spaces prenatally, 2) acidification of endolymph at postnatal day 10 (P10), 3) increased Ca<sup>2+</sup> concentration in the endolymph at P10, 4) reduction in endocochlear potential at P10, 5) loss of *Kcnj10* protein expression at P15, 6) macro-

phage invasion in stria vascularis at ~P35, 7) no changes in endolymphatic K<sup>+</sup> concentration in adult mice, and 8) degeneration of stria marginal cells in adult mice (12, 20, 42, 44).

In the cochlea, pendrin is mainly expressed in the apical membrane of outer sulcus and spiral prominence epithelial cells that border endolymph (Fig. 1) (14, 42). The observation that loss of pendrin leads to acidification of endolymph suggests that pendrin mediates HCO<sub>3</sub><sup>-</sup> secretion (28, 44).

Sensory transduction in the cochlea depends on the endocochlear potential, which is generated by the K<sup>+</sup> channel *Kcnj10* in stria vascularis (26, 41). The generation of a small endocochlear potential at P10 is consistent with the expression of K<sup>+</sup> channel *Kcnj10*. Both *Kcnj10* expression and endocochlear potential are lost during further development and consequently *Slc26a4*<sup>-/-</sup> mice never develop hearing (42, 44).

Loss of pendrin cannot directly affect *Kcnj10* protein expression, since *Kcnj10* and pendrin are expressed in different cells in the cochlear lateral wall (Fig. 1A) (42, 44). In this study, we hypothesize that free radical stress could be the link between loss of pendrin and reduction of *Kcnj10* protein expression.

Increased oxidative stress in the Pendred syndrome mouse model may be a consequence of enlarged endolymphatic spaces and/or the acidic endolymph. The K<sup>+</sup> concentration is maintained at normal levels in the enlarged *Slc26a4*<sup>-/-</sup> endolymph volume, which implies increased rates of K<sup>+</sup> secretion by stria vascularis to compensate for K<sup>+</sup> leakage (42). The rate of ion transport correlates with ATP production and metabolism in stria vascularis (23, 25). Elevated rates of K<sup>+</sup> secretion in the stria vascularis of *Slc26a4*<sup>-/-</sup> mice could enhance free radical stress as a result of increased energy metabolism, which is a major source of oxygen free radicals. Oxidative stress in stria vascularis may also be a consequence of endolymph acidification. The acidic pH of endolymph could reduce the cytosolic pH in stria marginal cells that border endolymph. Cytosolic acidification is a condition favorable to release of iron from proteins and in the presence of superoxide anion (O<sub>2</sub><sup>•-</sup>), nitric oxide radical (•NO) leads to the formation of peroxynitrite (ONOO<sup>-</sup>) and hydroxyl radical (•OH) (4, 10).

Oxygen free radicals can originate from a leaky electron transfer in the mitochondrial electron transport chain during production of ATP. Incomplete reduction of O<sub>2</sub> during metabolism generates the free radical (O<sub>2</sub><sup>•-</sup>), which spontaneously dismutates to hydrogen peroxide (H<sub>2</sub>O<sub>2</sub>). These two reactive oxygen species can be involved in further reactions that generate more aggressive, damaging radicals. In the presence of Fe<sup>2+</sup>, H<sub>2</sub>O<sub>2</sub> can enter into the Fenton reaction that yields the

Address for reprint requests and other correspondence: P. Wangemann, Anatomy and Physiology Dept., Kansas State Univ., 205 Coles Hall, Manhattan, KS 66506 (e-mail: wange@vet.ksu.edu).

The costs of publication of this article were defrayed in part by the payment of page charges. The article must therefore be hereby marked "advertisement" in accordance with 18 U.S.C. Section 1734 solely to indicate this fact.

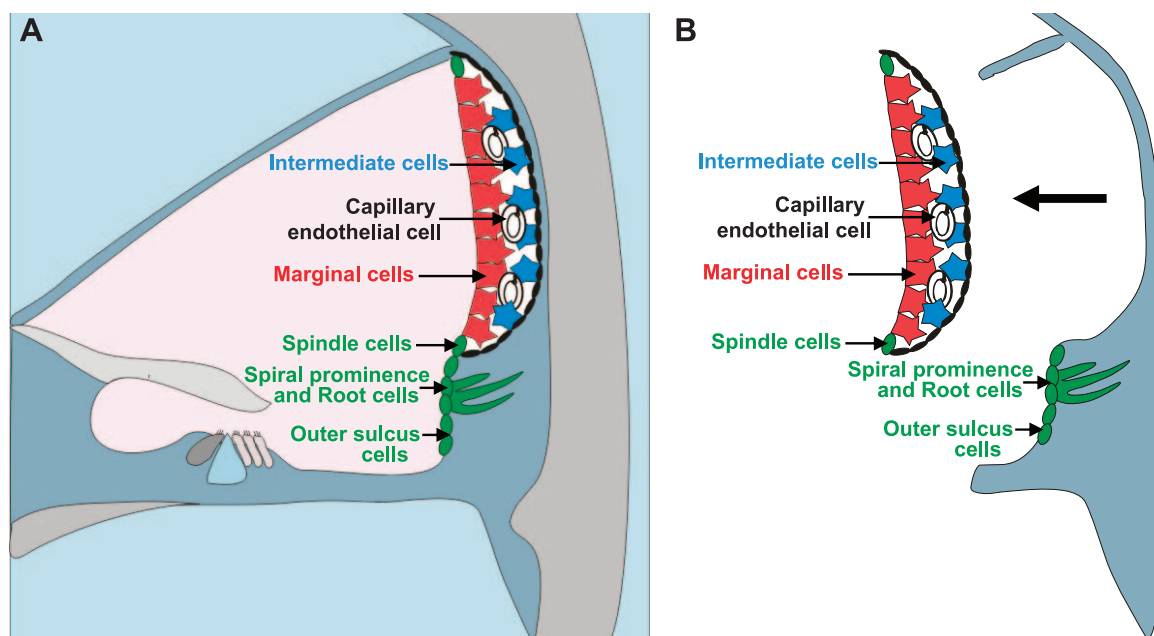


Fig. 1. Schematic diagram for *Kcnj10* and pendrin expression in the cochlea. *A*: *Kcnj10* is expressed in intermediate cells (blue) inside stria vascularis and pendrin is mainly expressed in spiral prominence epithelial cells, root cells, and in outer sulcus epithelial cells (green). *B*: 2 preparations were obtained from the lateral wall of the cochlea. The preparation of stria vascularis contained the  $K^+$  channel *Kcnj10* and the preparation of spiral ligament contained pendrin in cells located in spiral prominence epithelial cells, root cells, and in outer sulcus epithelial cells. Both *Kcnj10* and pendrin are lost in *Slc26a4*<sup>-/-</sup> mice. The preparation of spiral ligament also contained remnants of Reissner's membrane in addition to the spiral ligament.

extremely aggressive  $\cdot\text{OH}$ .  $\cdot\text{NO}$  synthesized by nitric oxide synthase can react with  $\text{O}_2^{\cdot-}$  to yield peroxynitrite ( $\text{ONOO}^-$ ) which decomposes to form  $\cdot\text{OH}$  and nitrate radical ( $\cdot\text{NO}_2$ ) (5, 40). Transition metal ions bound to lipids and proteins can react with  $\text{H}_2\text{O}_2$ ,  $\cdot\text{OH}$ , and  $\cdot\text{NO}_2$  to generate intermediates that subsequently cause oxidation and nitration of proteins and lipids, impairing the ability of the cell to function normally (30, 38).

Defense mechanisms against free radical stress entail sequestration of catalysts that promote the formation of free radicals and detoxification by chemical conversion. The free radical  $\text{O}_2^{\cdot-}$  can be converted to  $\text{O}_2$  and  $\text{H}_2\text{O}$  by superoxide dismutase in conjunction with catalase or glutathione peroxidase. Catalysts that generate free radicals, such as Fe, Zn, and Cu, are sequestered by ferritin, metallothionein, and ceruloplasmin (34, 36, 46). The cellular availability of the catalyst Fe is controlled via transcriptional and translational mechanisms. The expression of the Fe chelator transferrin (*Trf*) and the uptake mechanism transferrin receptor (*Tfrc*) are controlled by an iron-response protein, aconitase (*Aco1*) (8, 11). When the cytosolic free Fe concentration is high, retardation of *Tfrc* mRNA degradation is lifted and translation of *Trf* is promoted leading to an increased expression of the chelator *Trf* and a decreased expression of the Fe uptake mechanism *Tfrc*. Together, these changes in the expression of Fe-related proteins can mediate a reduction in the cytosolic free Fe concentration. Decreases in *Tfrc* transcript and increases in *Trf* protein expression, however, are often not sufficient to control oxidative stress and can be taken as an indication for the presence of Fe-mediated oxidative stress.

In the present study, we obtained direct and indirect measures of oxidative and nitrative stress before and after the onset of hearing in stria vascularis and a preparation of spiral ligament that included pendrin-expressing outer sulcus and

spiral prominence epithelial cells. The levels of oxidized and nitrated proteins in conjunction with the mRNA expression of genes involved in antioxidant defenses were used to assess oxidative and nitrative stress. We evaluated the impact of oxidative and nitrative stress on the protein levels of *Kcnj10* using an expression system model. To ascertain whether the loss of *Kcnj10* was a consequence of the conditions prevalent in the stria vascularis of *Slc26a4*<sup>-/-</sup> mice, stria vascularis from *P10* organ cultures and the corresponding time points in vivo were compared for the protein level expression of *Kcnj10*.

## METHODS

**Animal use and tissue preparations.** The *Slc26a4*<sup>-/-</sup> mouse strain was created in the laboratory of Dr. E. Green at the National Institutes of Health (12). *Slc26a4*<sup>-/-</sup> and *Slc26a4*<sup>+/-</sup> mice were raised in a colony at Kansas State University that was established with breeders kindly provided by Dr. S. Wall (Emory University). Mice were deeply anesthetized with tribromoethanol (560 mg/kg ip) and killed by transcardial perfusion with  $\text{Cl}^-$ -free solution.  $\text{Cl}^-$ -free solution contained (in mM) 150 Na-gluconate, 1.6  $\text{K}_2\text{HPO}_4$ , 0.4  $\text{KH}_2\text{PO}_4$ , 4  $\text{Ca}^{2+}$ -gluconate, 1  $\text{MgSO}_4$ , and 5 glucose, pH 7.4. Temporal bones housing the cochleae were removed and separate fractions of stria vascularis and spiral ligament were obtained by microdissection (Fig. 1B). All procedures concerning animals were approved by the Institutional Animal Care and Use Committee of Kansas State University.

**Quantitative RT-PCR.** Real-time RT-PCR in the presence of SYBR green (Molecular Probes, Eugene, OR) was carried out in 96-well plates (OneStep RT-PCR Kit, Qiagen Valencia, CA; iCycler, Bio-Rad, Hercules, CA) using gene-specific primers (Table 1). Transcripts were quantified in paired experiments using one master mix and total RNA isolated from pairs of age- and sex-matched *Slc26a4*<sup>-/-</sup> and *Slc26a4*<sup>+/-</sup> mice. RT was performed for 30 min at 50°C and terminated by heating to 95°C for 15 min. PCR consisted of 40 cycles of 1-min annealing at 60°C, 1-min elongation at 72°C, 20-s hot mea-

Table 1. *Gene-specific primers*

Gene	Primers	Product Size
Superoxide dismutase ( <i>Sod2</i> )	aca agc aca gcc tcc cag a (sense) tag cct cca gca act ct c (antisense)	291 bp
Metallothionein 3 ( <i>Mt3</i> )	gga tat gga ccc tga gac (sense) gac acc cag cac tat tta c (antisense)	260 bp
Aconitase ( <i>Aco1</i> )	cag gat gga tgc tac tac c (sense) gga ggt gct tgg taa tgg (antisense)	232 bp
Transferrin ( <i>Trf</i> )	act gct ctg cct tga caa tac (sense) cac gcc ttc ctg ctg att c (antisense)	319 bp
Transferrin receptor ( <i>Trfr</i> )	ttc cgc cat ct c agt cat cag (sense) tgg act tcg ccg caa cac (antisense)	300 bp
Ferritin ( <i>Ftl1</i> )	agc gtc tcc tcg agt ttc ag (sense) agg ttg gtc aga tgg ttg c (antisense)	200 bp

surement at 78°C, and 1-min denaturation at 94°C. Amplification of a single product was verified by gel electrophoresis and identity of the product was verified once by sequencing. The number of template molecules (T) was calculated according to  $T = 10^{\Delta \log(\text{number of molecules at Ct})/(\text{PCR efficiency} \times \Delta \text{Ct})}$ . Ct was defined as the cycle at which the fluorescence of the product molecules reached a set threshold. The number of molecules at Ct was calibrated by amplifying known numbers of 18S rRNA molecules. The content of 18S in total RNA was estimated under the assumption that total RNA consists of 100% of 18S and 28S rRNA. PCR efficiency was obtained from the slope of the log-linear phase of the growth curve (31).

**Isolation of protein.** Tissue fractions were transferred from the dissection dish into 0.5-ml Eppendorf tubes and Cl<sup>-</sup>-free solution was removed after a pulse spin. Four different methods for protein isolation were used. In *method 1*, proteins were extracted by first adding 20  $\mu$ l protein extraction *buffer 1* (ReadyPrep Sequential Extraction Kit, cat. no. 163–2101 and 163–2102, Bio-Rad) and vortexing for 3 min. The homogenized tissue was centrifuged at 16,000 rpm for 10 min at room temperature. Subsequently, extraction *buffer 2* was added and the process was repeated. Proteins in the supernatant were transferred into a new tube and either used immediately or stored at –80°C. In *method 2*, proteins were extracted by adding 30  $\mu$ l of Tris-Triton buffer (50 mM Tris, 150 mM NaCl, 1% Triton-X) and incubating for 30 min in a sonicating water bath at 0°C (Fisher Scientific FS20). Proteins in the supernatant were transferred to a new tube and either used immediately or stored at –80°C. In *method 3*, proteins were extracted by adding 30  $\mu$ l of Tris-SDS buffer (50 mM Tris, 150 mM NaCl, 0.5% SDS) and incubating for 30 min in a sonicating water bath at 0°C. Proteins in the supernatant were transferred to a new tube and either used immediately or stored at –80°C. In *method 4*, the tissue was fixed in 0.6 N trichloroacetic acid on ice, centrifuged at 15,000 rpm for 10 min at 4°C, and the supernatant was removed. The proteins were extracted by adding 30  $\mu$ l of urea buffer (9 M urea, 0.065 mM DTT, 2% Triton X-100) and incubating for 30 min in a sonicating water bath at 0°C. The protein-containing solution was neutralized by adding 1 M Tris. To this solution, 5  $\mu$ l of 1% SDS were added and resulting mixture was incubated for 30 min in a sonicating water bath at 0°C. Proteins in the supernatant were transferred to a new tube and either used immediately or stored at –80°C.

**Detection of oxidized proteins.** Carbonyl groups of oxidized proteins were derivatized with dinitrophenylhydrazine (Oxyblot Kit, cat. no. S7150, Millipore, Billerica) to form dinitrophenylhydrazone (DNP). DNP-labeled proteins were separated by SDS gel electrophoresis (5  $\mu$ l/lane) and detected in Western blots. Procedures were carried out according to the manufacturer's recommendations. Differences in the presence of oxidized proteins were evaluated by comparison to the expression of actin or tubulin.

**Quantitation of nitrated proteins by ELISA.** Protein was isolated using the Tris-Triton method (*method 2*) and the level of nitration was quantified by two different immunoabsorbent assays (cat. no. HK501,

Cell Sciences, Canton, MA; cat. no. 17-376, Millipore) according to the manufacturer's recommendation. The total protein content of the sample was measured (NanoOrange protein quantitation kit, cat. no. N666, Invitrogen, Carlsbad, CA). Differences in the amount of nitrated proteins were evaluated by comparison of nitrated protein content to the total protein content.

**Quantitative Western blotting.** An equal volume of Laemmli buffer containing 5%  $\beta$ -mercaptoethanol was added to the protein samples and incubated at 75°C for 10 min. Protein samples (15  $\mu$ l) were separated by SDS-PAGE gel electrophoresis (4–15% Tris-SDS Polyacrylamide Precast Gels, Bio-Rad). After separation, proteins were transferred to either nitrocellulose or PVDF membranes (0.2- $\mu$ m-pore size, Bio-Rad), blocked with 5% dry milk in TBS-Tween (137 mM NaCl, 20 mM Tris-HCl, 0.1% Tween 20, pH 7.6), and probed with primary antibodies (rabbit anti-*Kcnj10*, 1:1,000, cat. no. APC-035, Alomone Labs, Jerusalem, Israel; mouse anti-*Kcnj10*, cat. no. H00003766-M01, Novus Biologicals, Littleton, CO; rabbit anti-*trf*, 1:750, cat. no. A76, Biomed, Foster City, CA; mouse anti-*trfc*, 1:2,000, cat. no. 13-6800, Zymed, San Francisco, CA; rabbit anti-actin, 1:1,000, cat. no. A2066, Sigma, St. Louis, MO; rabbit anti-tubulin, 1:500, cat. no. ab6046, Cambridge, MA). Membranes were washed 4 $\times$  for 15 min in TBS-Tween and incubated with horseradish peroxidase (HRP)-conjugated secondary antibodies (anti-rabbit, 1:10,000, cat. no. 1858415; anti-mouse, 1:10,000, cat. no. 1858416, Pierce, Rockford, IL). After being washed 4 $\times$  for 15 min in TBS-Tween, HRP was detected by chemiluminescence (SuperSignal West Femto Maximum Sensitivity Substrate, cat. no. 34095, Pierce) using a camera-based imaging workstation (4000MM, Kodak). Quantification of oxidized proteins and of *Kcnj10* protein was carried out by integration of signals arising from specific staining (Fig. 2). Differences in *Kcnj10* expression were evaluated by comparison to the expression of actin or tubulin.

**Immunoprecipitation.** Protein was isolated using the Tris-Triton method (*method 2*). An equal volume of sepharose protein G beads (cat. no. P3296, Sigma) was added to protein lysate followed by incubation on ice for 60 min. This mixture was spun at 10,000 g for 10 min at 4°C and the supernatant (precleared lysate) was transferred to a fresh Eppendorf tube. Ten micrograms of mouse monoclonal antibody for *Kcnj10* were added to the cold precleared lysate and the mixture was incubated at 4°C for 1 h. Fifty microliters of protein G beads washed in Tris-Triton buffer were added to the antibody-lysate mixture followed by incubation for 3 h at 4°C on a shaker. The supernatant was removed after a quick spin (10,000 g for 30 s) and the beads were washed 4 $\times$  in Tris-Triton buffer. Fifty microliters of 1 $\times$  Laemmli buffer were added to the bead pellet and this mixture was



Fig. 2. Illustration of the method used for the quantification of oxidized proteins and of *Kcnj10* protein expression. Chemiluminescence was detected as digital format using a camera-based system (Kodak 4000 MM). Staining, consisting of both smears and bands, was observed for oxidized proteins as well as for *Kcnj10* protein. The specificity of smears and bands was confirmed in independent experiments. The intensity of staining was integrated over the entire length of the blot.

vortexed and heated at 95°C for 15 min followed by centrifugation at 10,000 *g* for 5 min. The supernatant was collected in a fresh Eppendorf tube and used as the sample for Western blotting.

**Quantification of total tissue Fe content.** Total tissue Fe content (tissue-Fe) was measured using a modified ferrozine-based assay (15). Freshly isolated tissue fractions of stria vascularis and spiral ligament were transferred into Eppendorf tubes and  $\text{Cl}^-$ -free solution was removed. Guanidine hydrochloride (2  $\mu\text{l}$ ) was added to the tissue and mixing was facilitated by a pulse spin. After incubation for 45 min at 60°C, 2  $\mu\text{l}$  of FAT solution were added. FAT solution contained 0.5 M ferrozine, 0.5 M ascorbic acid, and 1 M Tris·HCl, pH 7. Mixing was facilitated by a pulse spin and the tissue was incubated for 45 min at 60°C. Absorbance at 562 nm was measured in the supernatant of the 4- $\mu\text{l}$  sample (ND1000, Nanodrop Technologies) and standards containing  $\text{FeCl}_2$  that were processed in parallel. Following tissue-Fe measurements, the total protein content of samples was determined (NanoOrange Protein Quantitation Kit). Measurements of the tissue-Fe are reported per milligram of protein.

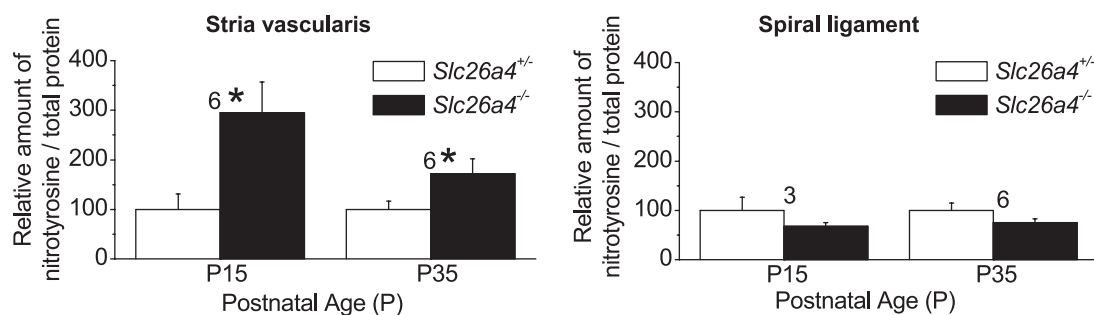
**Organ culture.** Freshly microdissected stria vascularis from *P10 Slc26a4<sup>+/-</sup>* and *Slc26a4<sup>-/-</sup>* mice was cultured in 35-mm flat-bottom culture dishes (cat. no. 08-757-100A, Fisher) containing 2 ml media for 1, 3, and 5 days. The media consisted of DMEM (cat. no. 30-2002, ATCC) supplemented with 10% FBS (cat. no. 30-2020, ATCC), 500  $\mu\text{M}$  furosemide (cat. no. F4381, Sigma), and 1% penicillin-streptomycin antibiotic mixture. The media was changed every day. Cultured stria vascularis at the end of 1, 3, and 5 days was transferred from the culture dish to a 0.5-ml Eppendorf tube and washed twice with  $\text{Cl}^-$ -free solution to remove excess media. Protein was isolated using

the Tris-Triton buffer (*method 3*). Protein was either used immediately or stored at -80°C.

**Cell culture.** Chinese hamster ovary cells (CHO)-K1 (cat. no. CRL-9618, ATCC, Manassas, VA) were cultured as monolayers in DMEM supplemented with 10% FBS and 1% penicillin-streptomycin antibiotic mixture (cat. no. 30-2300, ATCC) in a cell culture incubator maintained at 37°C and 5%  $\text{CO}_2$ . The CHO-K1 cells were transfected in a T25 flask (cat. no. 10-126-39, Fisher, St. Louis, MO) with a GFP-*Kcnj10*-Export sequence plasmid (a generous gift from Dr. N. Klocker, Dept. of Physiology, University of Freiburg, Germany) using Lipofectamine 2000 (cat. no. 11668-019, Invitrogen) according to the manufacturer's instructions. The CHO-K1 cells containing the GFP-*Kcnj10*-Export plasmid were split 24 h posttransfection and seeded in three wells. To replicate the conditions of organ culture, 500  $\mu\text{M}$  furosemide was added to each well 48 h posttransfection and wells were subjected to different levels of oxidative and nitrate stress. The first of the three wells was exposed to oxidative stress by adding 10  $\mu\text{M}$   $\text{H}_2\text{O}_2$  (cat. no. H1009, Sigma). The second well was exposed to oxidative and nitrate stress by adding 1 mM SIN-1 hydrochloride (cat. no. M5793, Sigma). The third well served as a control. This protocol was devised to ensure that differences in transfection efficiency did not impact the results. After 12 h, cells were lysed and protein was extracted using the Tris-Triton buffer. Protein was either used immediately or stored at -80°C.

**Statistical analysis.** Data are expressed as means  $\pm$  SE. Data were compared by paired and unpaired *t*-test as appropriate. Significance was assumed at  $P < 0.05$ .

## A Nitrated proteins



## B Oxidized proteins

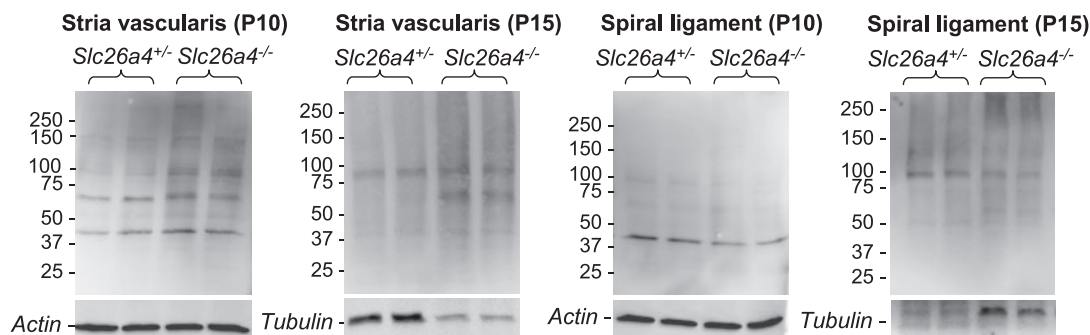


Fig. 3. Quantification of nitrated and oxidized proteins. **A:** nitrated proteins were quantified against total protein in stria vascularis and in the preparation of spiral ligament in *Slc26a4<sup>+/-</sup>* and *Slc26a4<sup>-/-</sup>* mice at ages postnatal day 15 (*P15*) and *P35*. Data are presented as percent of nitrated protein in stria vascularis of *Slc26a4<sup>+/-</sup>* mice. Significant changes are marked (\*) and numbers next to the bars represent the number of experiments. **B:** oxidized proteins were quantified against actin or tubulin in stria vascularis and in the preparation of spiral ligament in *Slc26a4<sup>+/-</sup>* and *Slc26a4<sup>-/-</sup>* mice at ages *P10* and *P15*. Representative examples of 3 experiments are shown. Increased amounts of nitrated and oxidized proteins were found in stria vascularis but not in the preparation of spiral ligament of *Slc26a4<sup>-/-</sup>* mice. The presence of nitrated and oxidized proteins indicates increased nitrate and oxidative stress in stria vascularis.

## RESULTS

*Stria vascularis contains elevated levels of nitrated proteins.* The amount of nitrated proteins in relationship to the total protein was quantified at ages *P15* and *P35* in stria vascularis and the spiral ligament preparation of *Slc26a4*<sup>-/-</sup> and *Slc26a4*<sup>+/-</sup> mice (Fig. 3A). Increased levels of nitration were observed in stria vascularis but not in the spiral ligament preparation of *Slc26a4*<sup>-/-</sup> compared with *Slc26a4*<sup>+/-</sup> mice. The increased levels of nitrated proteins suggest that stria vascularis of *Slc26a4*<sup>-/-</sup> mice is under increased nitrative stress.

*Stria vascularis contains elevated levels of oxidized proteins.* The presence of oxidized proteins was evaluated at *P10* and *P15* in the stria vascularis and the spiral ligament preparation of *Slc26a4*<sup>-/-</sup> and *Slc26a4*<sup>+/-</sup> mice (Fig. 3B). Detection of oxidized proteins involved DNP-labeling of carbonyl groups in oxidized proteins by derivatization with DNP. DNP-labeled proteins were detected by Western blot. No labeling was observed in the absence of derivatization. The levels of oxidized proteins were increased in stria vascularis but not in the spiral ligament preparation of *Slc26a4*<sup>-/-</sup> compared with *Slc26a4*<sup>+/-</sup> mice. The increased levels of oxidized proteins indicate that stria vascularis of *Slc26a4*<sup>-/-</sup> mice is under increased oxidative stress.

*Antioxidant defenses are reduced in stria vascularis.* Transcripts coding for superoxide dismutase (*Sod2*) and metallothionein (*Mt3*) were quantified in stria vascularis and in the spiral ligament preparation of *Slc26a4*<sup>-/-</sup> and *Slc26a4*<sup>+/-</sup> mice (Fig. 4). Expression of *Sod2* was reduced in stria vascu-

laris of *Slc26a4*<sup>-/-</sup> mice at ages *P10* and *P30*. Furthermore, transcripts for *Mt3* were reduced in stria vascularis of *Slc26a4*<sup>-/-</sup> mice at *P15*. No changes in expression of *Sod2* and *Mt3* were found in spiral ligament. These observations suggest that defenses against free radical stress are weakened in stria vascularis of *Slc26a4*<sup>-/-</sup> mice before and after the onset of hearing.

*Altered iron metabolism in stria vascularis is consistent with oxidative stress.* Transcripts were quantified in stria vascularis and in the spiral ligament preparation of *Slc26a4*<sup>+/-</sup> and *Slc26a4*<sup>-/-</sup> mice (Fig. 5). Transcripts included the Fe uptake mechanism transferrin receptor (*Tfrc*), the Fe chelator transferrin (*Trf*), the Fe storage protein ferritin (*Ftl1*), and the expression regulator iron-responsive protein (*Aco1*). Quantifications were performed before (*P10*) and after the onset of hearing (*P15*), after weaning (*P30–P35*), and in adulthood (*P75*). The numbers of transcripts coding for *Tfrc* were found to be reduced in *Slc26a4*<sup>-/-</sup> mice and this reduction was observed in stria vascularis at all ages including *P10*, and in the spiral ligament preparation at *P75*. The number of transcripts coding for *Trf* was elevated in *Slc26a4*<sup>-/-</sup> mice compared with *Slc26a4*<sup>+/-</sup> mice and this elevation was observed in stria vascularis from *P35* onward but not in the spiral ligament preparation. Transcripts for *Ftl1* were found reduced in number and this reduction was seen in stria vascularis from *P15* onward and in the spiral ligament preparation at *P10* and at *P75*. In addition, transcripts for *Aco1* were present in stria vascularis and spiral ligament of *Slc26a4*<sup>+/-</sup> and *Slc26a4*<sup>-/-</sup> mice. No difference in the number of transcripts was seen in stria vascularis of *Slc26a4*<sup>-/-</sup> compared with *Slc26a4*<sup>+/-</sup> mice; however, transcripts in the spiral ligament preparation were reduced at *P15* and at *P75*.

Protein expression of *Trf* and *Tfrc* was quantified at age *P35* in stria vascularis and the spiral ligament preparation of *Slc26a4*<sup>+/-</sup> and *Slc26a4*<sup>-/-</sup> mice (Fig. 6). Protein expression of *Trf* was increased and protein expression of *Tfrc* was decreased in stria vascularis but not in the spiral ligament preparation of *Slc26a4*<sup>-/-</sup> mice compared with *Slc26a4*<sup>+/-</sup> mice. The increase in *Trf* expression is consistent with the increase in *Trf* transcripts (Fig. 5) and with *Aco1*-mediated translational expression regulation via an elevated free Fe pool. The decrease in *Tfrc* expression is consistent with the observed decrease in transcripts and *Aco1*-mediated transcriptional regulation via an elevated free Fe pool.

Tissue-Fe was measured at age *P10*, before the onset of hearing, in stria vascularis and the spiral ligament preparation of *Slc26a4*<sup>+/-</sup> and *Slc26a4*<sup>-/-</sup> mice (Fig. 6). No difference in tissue-Fe was found in stria vascularis and spiral ligament of *Slc26a4*<sup>-/-</sup> compared with *Slc26a4*<sup>+/-</sup> mice.

The changes in the transcript and protein level expression of *Trf* and *Tfrc* indicate Fe-mediated oxidative stress in the stria vascularis of *Slc26a4*<sup>-/-</sup> mice. The reduction in *Ftl1* transcripts is consistent with a reduced capacity to sequester Fe and weakened defenses against oxidative stress.

*Western blot for Kcnj10 protein in stria vascularis.* Before evaluating the effect of oxidative and nitrative stress on *Kcnj10* protein expression, the specificity of *Kcnj10* antibodies was evaluated. Western blots revealed a considerable interexperimental variability in the pattern of bands and smears detected by anti-*Kcnj10* antibodies. Reprobing individual blots with two different anti-*Kcnj10* antibodies, one of which was a mono-

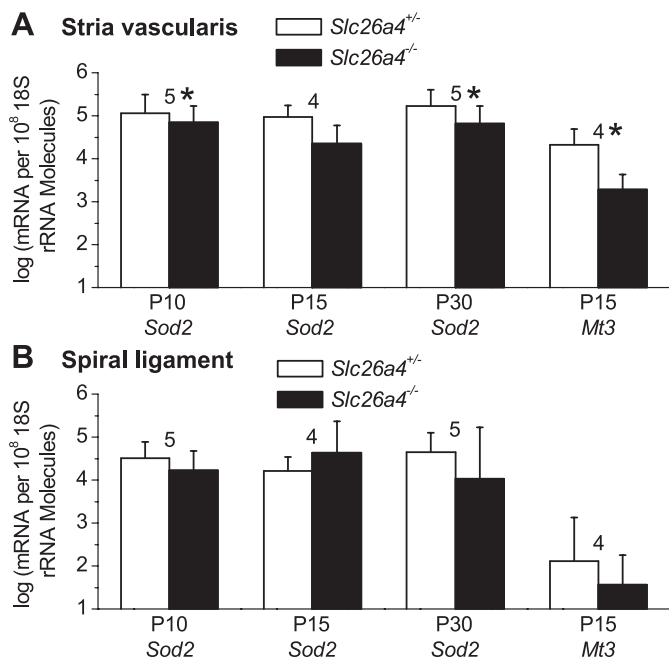


Fig. 4. Quantification of transcripts coding for free radical defenses. A and B: transcripts coding for superoxide dismutase (*Sod2*) and metallothionein (*Mt3*) were quantified relative to 18S in stria vascularis and in the preparation of spiral ligament from *Slc26a4*<sup>+/-</sup> and *Slc26a4*<sup>-/-</sup> mice at age *P10*, *P15*, and *P30*. Significant changes are marked (\*) and numbers next to the data represent the number of animal pairs. Reductions in the number of transcripts, which indicates weakened defenses against free radical stress, were seen in stria vascularis but not in spiral ligament.

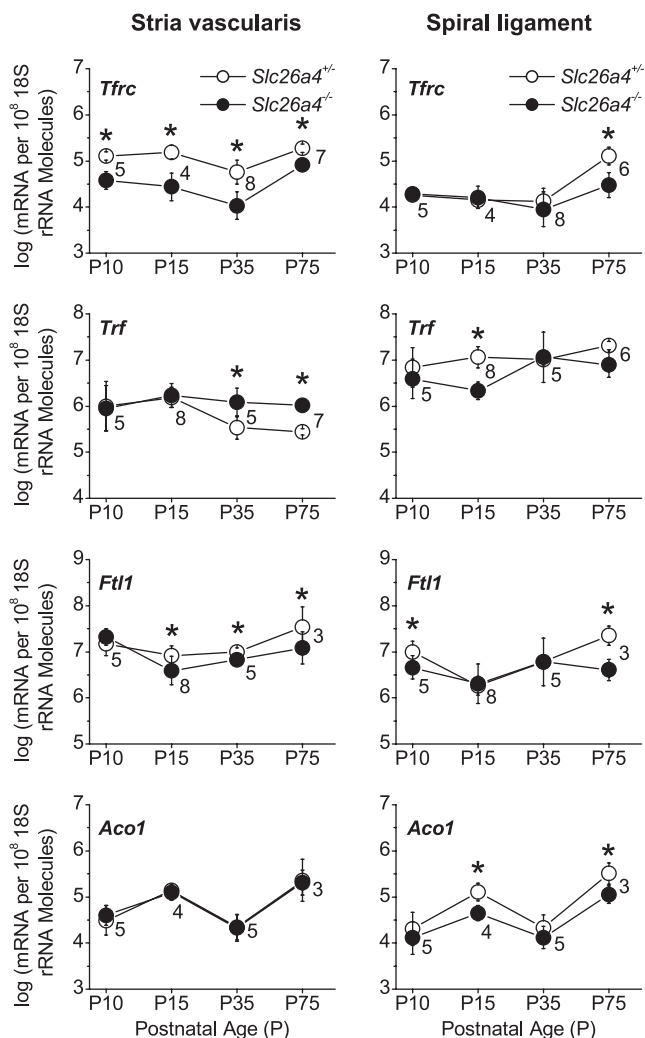


Fig. 5. Quantification of transcripts coding for proteins involved in Fe metabolism. Transcripts coding for transferrin receptor (*Tfrc*), transferrin (*Trf*), ferritin (*Ftl1*), and Fe-responsive protein (*Aco1*) were quantified relative to 18S in stria vascularis (left) and in the preparation of spiral ligament (right) of *Slc26a4*<sup>+/+</sup> and *Slc26a4*<sup>-/-</sup> mice at different ages. Significant changes are marked (\*) and numbers next to the data represent the number of animal pairs. The legend given pertains to all graphs. Reductions in *Tfrc* and *Ftl1* transcripts were mainly seen in stria vascularis. The reduction in *Tfrc* transcripts is consistent with an elevated pool of free Fe and *Aco1*-regulated degradation of *Tfrc* mRNA and the reduction in *Ftl1* transcripts is consistent with a reduced capacity to sequester Fe and Fe-mediated free radical stress.

clonal, revealed highly similar patterns of bands and smears (Fig. 7, A vs. C and D vs. F). Differences in the pattern of bands and smears were a function of the protein extraction method. The interexperimental variability, however, was encountered with all methods of protein extraction (compare Fig. 7, C and D). Immunoprecipitation with the mouse monoclonal and detection with the rabbit polyclonal antibody revealed monomers of *Kcnj10* at ~40 kDa as well as higher molecular weight bands and smears (Fig. 7G). This observation confirmed that the mouse monoclonal and the rabbit polyclonal antibody recognized the same protein in samples from stria vascularis.

Furthermore, incubating the primary antibody with a blocking peptide (KLEESLREQAEGKSALSVR) resulted in the loss of all bands and smears (Fig. 7, H and I). In this experi-

ment, a single lane of a blot was probed for *Kcnj10* protein using the rabbit polyclonal antibody and then stripped and cut into two pieces that were re probed for *Kcnj10* in the absence and presence of blocking peptide. The cut pieces were rejoined for detection. This experimental protocol was chosen to unambiguously demonstrate that the addition of blocking peptide is sufficient to prevent detection of *Kcnj10*. Taken together, these data verify that the rabbit polyclonal and the mouse monoclonal antibody detect *Kcnj10* and that *Kcnj10* in stria vascularis exists as monomers (~40 kDa), as well as in variable higher molecular weight complexes. In subsequent experiments both smears and bands were regarded as *Kcnj10* protein and quantification of expression was based on integrals of staining as shown in Fig. 2.

The variability in the pattern of *Kcnj10* expression is likely due to the interaction with the dystrophin glycoprotein complex. This complex contains proteins that greatly vary in their

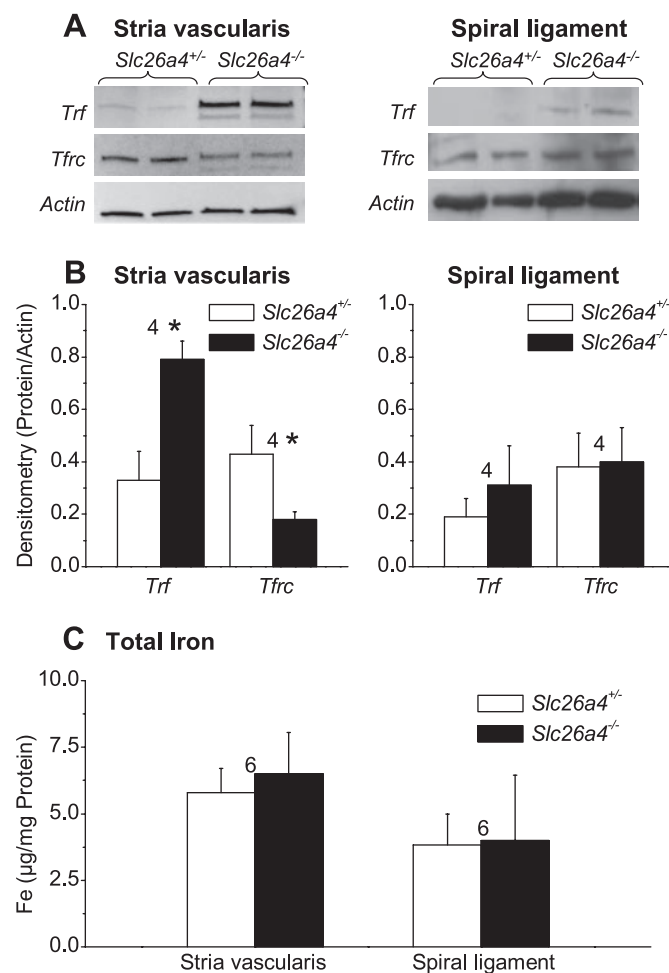


Fig. 6. Quantification of proteins involved in Fe metabolism and total iron. A and B: transferrin (*Trf*) and transferrin receptor (*Tfrc*) were quantified relative to actin in stria vascularis and in the preparation of spiral ligament of *Slc26a4*<sup>+/+</sup> and *Slc26a4*<sup>-/-</sup> mice at age P35. Representative Western blots and data summaries are shown. Significant changes are marked (\*) and numbers next to the bars represent the number of blots. Changes in protein expression were seen in stria vascularis but not in the preparation of spiral ligament. C: tissue-Fe was quantified in stria vascularis and spiral ligament of *Slc26a4*<sup>+/+</sup> and *Slc26a4*<sup>-/-</sup> at age P10. No difference was found in tissue-Fe. The increase in *Trf* protein expression and the reduction in *Tfrc* protein expression are consistent with Fe-mediated free radical stress.

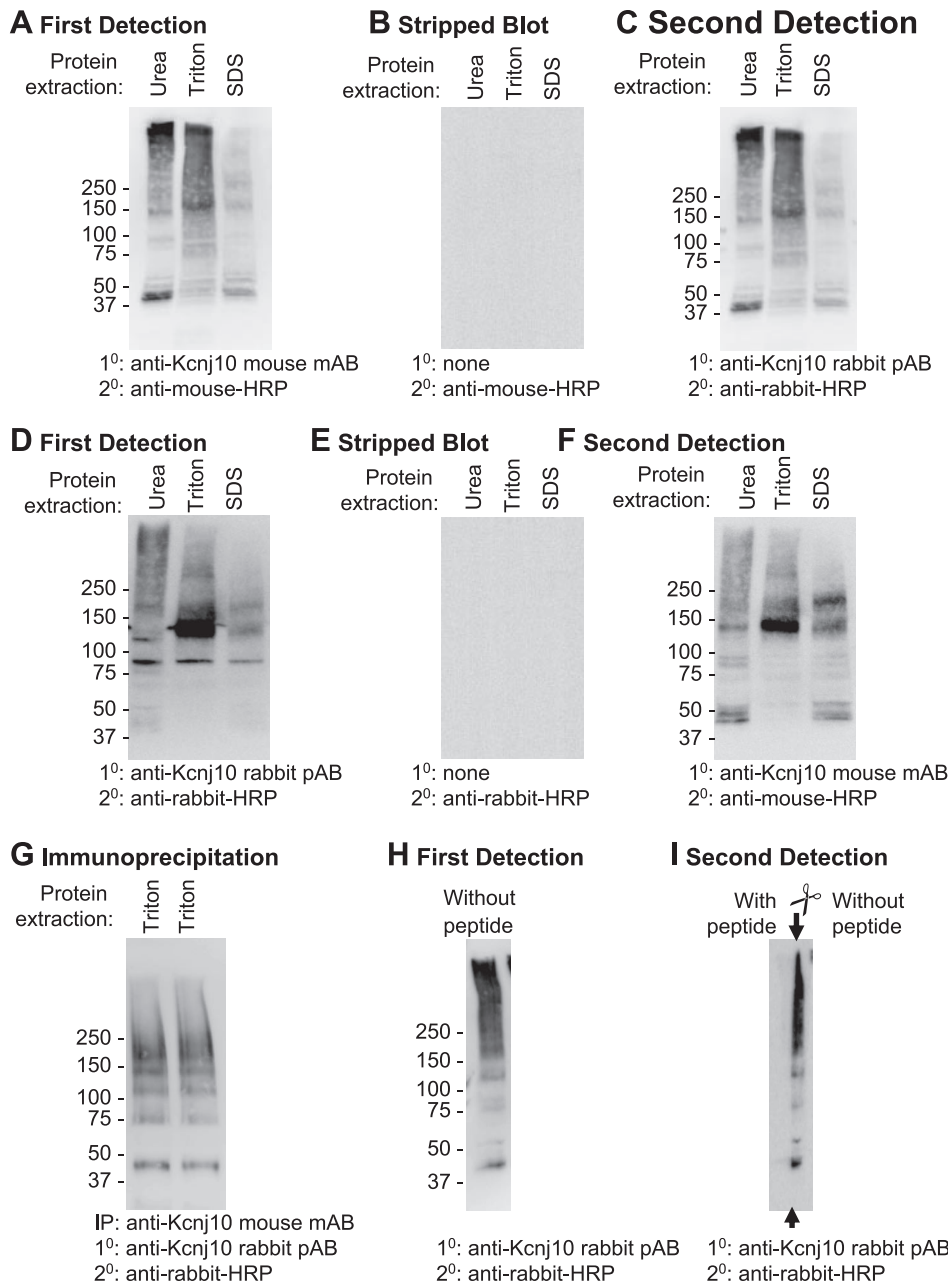


Fig. 7. Western blot for *Kcnj10* protein in stria vascularis. A–C: protein was extracted from stria vascularis using 3 different methods and first probed for *Kcnj10* with a mouse monoclonal antibody. This blot was stripped and re-probed for *Kcnj10* with a rabbit polyclonal antibody. Note that the pattern of staining varied with the method of extraction but not with the antibody used for probing (compare A and C). D–F: similar experiments were performed in reverse order. Protein was extracted from stria vascularis using 3 different methods and first probed for *Kcnj10* with a rabbit polyclonal antibody. The blot was then stripped and re-probed for *Kcnj10* with a mouse monoclonal antibody. Note that considerable interexperimental variability in the pattern of bands and smears was encountered (compare C and D) but that the little variability was seen with the different antibodies (compare D and F). G: protein lysate from stria vascularis was immunoprecipitated with mouse monoclonal antibody for *Kcnj10* and the resulting Western blot was probed with a rabbit polyclonal antibody for *Kcnj10*. Note that a monomeric form of *Kcnj10* (~40 kDa) and complexes that resulted in bands and smears of higher molecular weight were observed by immunoprecipitation as well as by Western blotting of whole cell lysates (compare A and G). H and I: single lane containing stria vascularis protein was probed for *Kcnj10*, stripped, cut into 2 pieces (indicated by scissor symbol), and probed again for *Kcnj10* in the presence and absence of blocking peptide. These experiments confirmed that Western blot for *Kcnj10* in stria vascularis has both smears and bands.

mobility patterns due to variable glycosylations and stoichiometries. *Kcnj10* protein has been shown to be associated with the dystrophin glycoprotein complex in brain and retina and with aquaporin 4 in retina (6, 7). Moreover, ubiquitination may contribute to the observed smears.

**Progressive loss of *Kcnj10* expression in the stria vascularis of *Slc26a4*<sup>-/-</sup> mice.** Protein expression of *Kcnj10* was quantified in stria vascularis before the onset of hearing (P10 and P11) and after the onset of hearing (P13 and P15; Fig. 8). As expected, stria vascularis of *Slc26a4*<sup>+/-</sup> mice maintained and stria vascularis of *Slc26a4*<sup>-/-</sup> mice progressively lost the expression of *Kcnj10* protein. These results are consistent with previous studies showing loss of *Kcnj10* protein expression at P15 by immunohistochemistry and the loss of endocochlear potential (44). The loss of *Kcnj10* protein expression occurs at a time point when the stria vascularis of *Slc26a4*<sup>-/-</sup> mice is

under increased oxidative and nitrate stress. This finding suggests that increased oxidative and/or nitrate stress contributes to the loss of *Kcnj10* protein expression in the stria vascularis of *Slc26a4*<sup>-/-</sup> mice.

**Protocol development for organ culture of stria vascularis.** A previous study showed that stria vascularis in organ culture is poorly preserved and shows signs of degeneration in strial marginal and intermediate cells within 5 days (2). The degeneration of stria vascularis could be due to low apical concentration of K<sup>+</sup> in organ culture that would lead to elevated rates of K<sup>+</sup> secretion from strial marginal cells (43). Increased ion transport rates would increase ATP consumption, ATP production, and thereby enhance mitochondrial stress (25). Furosemide and furosemide analogs have been shown to reduce ATP consumption and inhibit K<sup>+</sup> secretion by strial marginal cells (23, 43). Reduced ATP consumption would reduce ATP

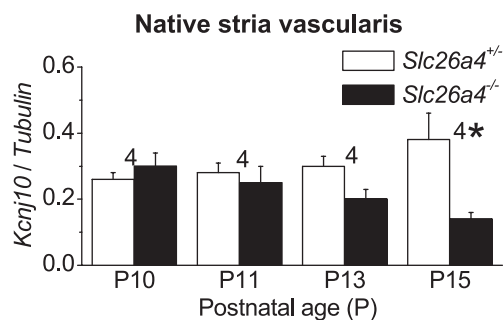


Fig. 8. Quantification of *Kcnj10* protein expression in native stria vascularis. Levels of *Kcnj10* protein were quantified against tubulin at P10, P11, P13, and P15. Significant changes between corresponding time points are marked (\*) and numbers next to the bars represent the number of experiments. *Kcnj10* expression was progressively lost from the stria vascularis of *Slc26a4*<sup>-/-</sup> mice. The loss of *Kcnj10* expression in native tissue that is under the influence of oxidative/nitrative stress supports a role for oxidative/nitrative stress-mediated loss of *Kcnj10* expression.

production and thereby lower oxidative stress. Therefore, furosemide supplementation might be useful in preserving the integrity of stria vascularis in organ culture. Stria vascularis was cultured in media with/without furosemide for 0, 1, 3, and 5 days and evaluated for viability by quantifying the levels of tubulin. In the absence of furosemide, tubulin expression was gradually lost. In the presence of furosemide, stria vascularis could be cultured for at least 5 days (Fig. 9). Therefore, to evaluate the expression of *Kcnj10* in organ culture, stria vascularis was cultured in media supplemented with furosemide.

Similar expression of *Kcnj10* in organ culture of *Slc26a4*<sup>-/-</sup> and *Slc26a4*<sup>+/-</sup> mice. Stria vascularis from P10 *Slc26a4*<sup>-/-</sup> and *Slc26a4*<sup>+/-</sup> mice were cultured. Protein expression of *Kcnj10*

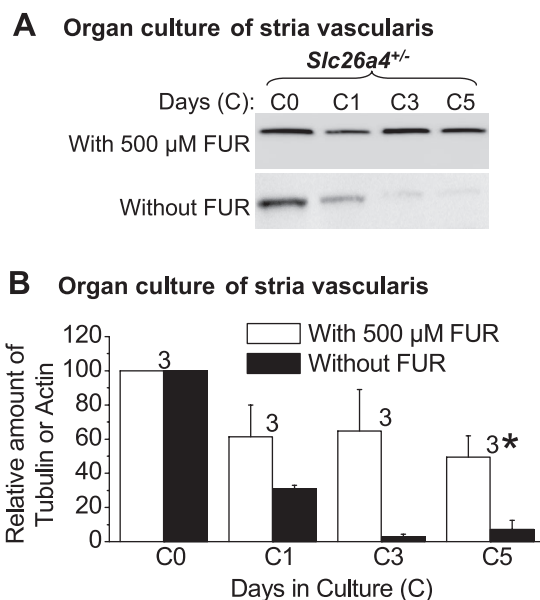


Fig. 9. Quantification of tubulin or actin protein expression in organ culture of stria vascularis. A and B: levels of tubulin or actin were quantified in P10 stria vascularis of *Slc26a4*<sup>+/-</sup> mice at 0, 1, 3, and 5 days in organ culture. Data are presented as percent of tubulin or actin protein at 0 day of culture, which corresponds to age P10. Significant changes between corresponding time points are marked (\*) and numbers next to the bars represent the number of experiments. Tubulin or actin expression was gradually lost in organ culture of stria vascularis in the absence of furosemide (FUR). Stria vascularis can be cultured for at least 5 days when the media is supplemented with 500 μM FUR.

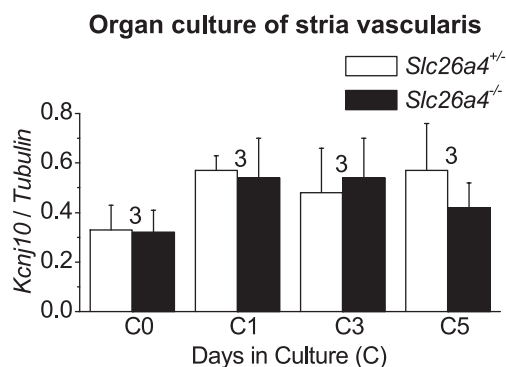


Fig. 10. Quantification of *Kcnj10* protein expression in organ culture of stria vascularis. Levels of *Kcnj10* protein were quantified against tubulin in P10 stria vascularis of *Slc26a4*<sup>+/-</sup> and *Slc26a4*<sup>-/-</sup> mice at 0, 1, 3, and 5 days in organ culture. Significant changes between corresponding time points are marked (\*) and numbers next to the bars represent the number of experiments. In contrast to native stria vascularis shown in Fig. 9, *Kcnj10* expression level in organ culture (shown here) followed the same trend in *Slc26a4*<sup>+/-</sup> and *Slc26a4*<sup>-/-</sup> mice. Similar levels of *Kcnj10* expression in stria vascularis of *Slc26a4*<sup>+/-</sup> and *Slc26a4*<sup>-/-</sup> mice under conditions of equal oxidative challenge in organ culture conditions support oxidative stress-mediated loss of *Kcnj10* expression.

was quantified in organ culture at 1, 3, and 5 days, corresponding to the time points of measurements in native tissue at P11, P13, and P15. Under conditions of equal oxidative stress in organ culture, stria vascularis of *Slc26a4*<sup>-/-</sup> mice was able to maintain *Kcnj10* expression at a level similar to *Slc26a4*<sup>+/-</sup> mice (Fig. 10). These observations suggest that oxidative stress mediates the loss of *Kcnj10* expression in the native tissue.

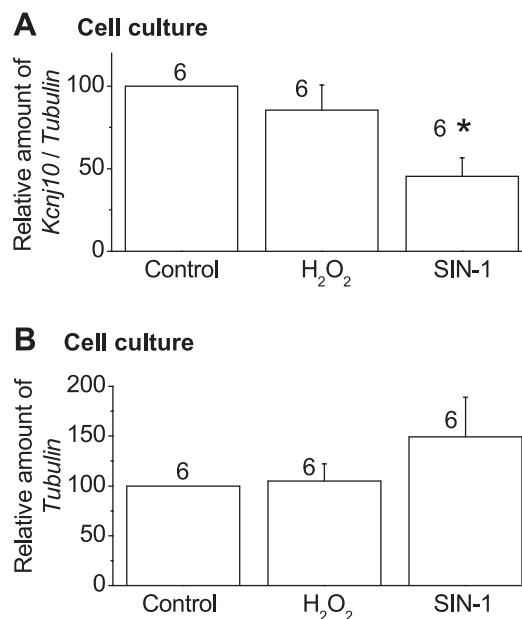


Fig. 11. Quantification of *Kcnj10* protein expression under free radical stress. A and B: levels of *Kcnj10* protein were quantified against tubulin in cell culture under the influence of 10 μM H<sub>2</sub>O<sub>2</sub> and 1 mM SIN-1. Data are presented as percent of *Kcnj10* expression in control samples. Decrease in the expression of *Kcnj10* protein was found in SIN-1-mediated oxidative and nitrative stress but not in H<sub>2</sub>O<sub>2</sub>-mediated oxidative stress. No significant change was found in the expression levels of tubulin between control and H<sub>2</sub>O<sub>2</sub> or SIN-1 treatments. The loss of *Kcnj10* expression under free radical stress provides a mechanism for the observed loss of *Kcnj10* in the stria vascularis of *Slc26a4*<sup>-/-</sup> mice.

*Loss of Kcnj10 protein expression under oxidative and nitritive stress.* The effect of oxidative and nitritive stress on protein expression of *Kcnj10* was evaluated in an heterologous expression system (Fig. 11). Cells were transfected with a vector that contains *Kcnj10-GFP-export-sequence*. This plasmid was used in our study because the localization of *Kcnj10* to plasma membrane in native tissues is lost under cell culture. However, insertion of the ER export sequence for Kir2.1 into the COOH terminal of *Kcnj10* enables it to translocate to the plasma membrane (39). Cells were treated with 500  $\mu$ M furosemide to replicate the conditions present in organ culture. Oxidative stress was induced by incubation with 10  $\mu$ M H<sub>2</sub>O<sub>2</sub>. Furthermore, oxidative and nitritive stress was induced by incubation with 1 mM SIN-1. SIN-1 releases equimolar amounts of O<sub>2</sub><sup>•-</sup> and •NO that react to produce peroxynitrite (27). *Kcnj10* expression was reduced in cells treated with SIN-1 but not in cells treated with H<sub>2</sub>O<sub>2</sub>. No significant change was found in the expression levels of tubulin suggesting that the observed differences in *Kcnj10* expression are not due to cell death or degeneration. SIN-1-mediated loss of *Kcnj10* suggests that free radical stress comprising both oxygen and nitrogen radicals is capable of reducing *Kcnj10* expression. It is conceivable that observed loss of *Kcnj10* expression in stria vascularis of *Slc26a4*<sup>-/-</sup> mice is due to the combined effect of oxidative and nitritive stress.

## DISCUSSION

The most salient findings of the present study are that 1) free radical stress is increased in stria vascularis of *Slc26a4*<sup>-/-</sup> mice as early as *P10*, which is before the onset of hearing; 2) *Kcnj10* expression is lost progressively in the stria vascularis of *Slc26a4*<sup>-/-</sup> mice; 3) under conditions of equal oxidative stress, stria vascularis of *P10 Slc26a4*<sup>-/-</sup> and *Slc26a4*<sup>+/-</sup> mice have a similar pattern of expression in organ culture; and 4) *Kcnj10* expression is reduced under free radical stress in cell culture. These results suggest that free radical stress is involved in the etiology of hearing loss in Pendred syndrome.

Free radical stress that exceeds the capacity of defense mechanisms has been implicated in inner ear pathogenesis including acoustic trauma and drug-induced ototoxicity (17, 33). Stria vascularis is prone to free radical stress due to its high metabolic activity and dense vascular system (25). Oxygen free radical (O<sub>2</sub><sup>•-</sup>) is a product of energy metabolism in the mitochondria and the nitrogen free radical (•NO) is generated by nitric oxide synthase in the endothelial cells of stria vascularis. The reaction between O<sub>2</sub><sup>•-</sup> and •NO produces peroxynitrite (ONOO<sup>-</sup>). ONOO<sup>-</sup> decomposes to form the very aggressive nitrate radical (•NO<sub>2</sub>), which causes nitration of proteins. The formation of •NO<sub>2</sub> from ONOO<sup>-</sup> is facilitated under acidic conditions or in the presence of CO<sub>2</sub> (5, 24). The sensitivity of *Kcnj10* protein expression to free radical stress and the presence of oxidative and nitritive stress in stria vascularis suggest that free radical stress is responsible for the loss of *Kcnj10* in Pendred syndrome.

Reduction of *Kcnj10* protein expression under free radical stress is a pathobiologic mechanism that is not limited to Pendred syndrome. Loss of *Kcnj10* under free radical stress is also implicated in other disease models. *Kcnj10* protein expression, unlike the expression of other K<sup>+</sup> channels, is reduced in the retina after ischemia-reperfusion injury, an insult that is

associated with oxidative stress (19). Furthermore, mice expressing a mutant superoxide dismutase (SOD1-G93A) have increased oxidative stress and reduced expression of *Kcnj10* protein in spinal cord tissues (1, 22).

The origin of increased free radical stress in stria vascularis may be related to the enlarged endolymphatic volume or the acidified endolymphatic pH of *Slc26a4*<sup>-/-</sup> mice. Enlargement of the cochlear and vestibular endolymphatic compartments develop in *Slc26a4*<sup>-/-</sup> mice prenatally after embryonic day 13 (*E13*), when the onset of pendrin expression fails to occur in *Slc26a4*<sup>-/-</sup> mice (12). Shortly after birth, the composition of endolymph changes from a Na<sup>+</sup>-rich fluid to a K<sup>+</sup>-rich fluid. The onset of K<sup>+</sup> secretion occurs at *P3* (3, 45). K<sup>+</sup> is secreted by stria vascularis and the rate of K<sup>+</sup> secretion is controlled by the endolymphatic K<sup>+</sup> concentration (41, 43). Enlarged endolymphatic spaces with an inherently less favorable surface-to-volume ratio may require larger rates of K<sup>+</sup> secretion to offset leakage and maintain the normal high endolymphatic K<sup>+</sup> concentration found in *Slc26a4*<sup>-/-</sup> mice (42). Higher rates of K<sup>+</sup> secretion can be associated with higher rates of oxidative stress since metabolism and ATP production in stria vascularis are tightly linked to the rate of ion transport (23, 25). It is conceivable that the onset of oxidative stress in stria vascularis coincides with the onset of K<sup>+</sup> secretion at *P3*, which is before the onset of *Kcnj10* expression and rise of endocochlear potential at *P8* and the onset of hearing at *P12* (3, 18, 35, 44).

Acidification of endolymph was observed in *Slc26a4*<sup>-/-</sup> mice at *P10* and older ages (28, 44). Acidification could contribute to free radical stress in stria vascularis if the lowered pH of endolymph would decrease the cytosolic pH of the adjacent stria marginal cells that are the most likely source of O<sub>2</sub><sup>•-</sup>. The cytosolic pH could induce oxidative stress by enhancing the stability of •OH and by promoting the formation of the aggressive •OH, •NO<sub>2</sub> from O<sub>2</sub><sup>•-</sup> and •NO (5, 10).

In conclusion, the data demonstrate that loss of pendrin leads to free radical stress in stria vascularis and that free radical stress is sufficient to cause the loss *Kcnj10* expression. The loss of *Kcnj10* expression in stria vascularis leads to the loss of the endocochlear potential and the failure to develop hearing in the mouse model of Pendred syndrome.

## ACKNOWLEDGMENTS

The authors are grateful to C. Linsenmeyer and S. Billings for genotyping animals and proofreading drafts of the manuscript.

## GRANTS

The support by National Institutes of Health Research Grants R01-DC-01098 and P20-RR-017686 (molecular biology and biochemistry core facility) is gratefully acknowledged. N. Gunhanlar from Bilkent University (Ankara, Turkey) participated in the development of Western blots during her 2006 summer internship in the laboratory.

## REFERENCES

1. Andrus PK, Fleck TJ, Gurney ME, Hall ED. Protein oxidative damage in a transgenic mouse model of familial amyotrophic lateral sclerosis. *J Neurochem* 71: 2041–2048, 1998.
2. Anniko M. The postnatal mammalian labyrinthine secretory epithelium in vitro. *Acta Otolaryngol (Stockh)* 90: 237–243, 1980.
3. Anniko M, Nordemar H. Embryogenesis of the inner ear. IV. Postnatal maturation of the secretory epithelia of the inner ear in correlation with the elemental composition in the endolymphatic space. *Arch Otorhinolaryngol* 229: 281–288, 1980.

4. Balagopalakrishna C, Paka L, Pillarisetti S, Goldberg IJ. Lipolysis-induced iron release from diferric transferrin: possible role of lipoprotein lipase in LDL oxidation. *J Lipid Res* 40: 1347–1356, 1999.
5. Beckman JS, Beckman TW, Chen J, Marshall PA, Freeman BA. Apparent hydroxyl radical production by peroxynitrite: implications for endothelial injury from nitric oxide and superoxide. *Proc Natl Acad Sci USA* 87: 1620–1624, 1990.
6. Connors NC, Adams ME, Froehner SC, Kofuji P. The potassium channel Kir4.1 associates with the dystrophin-glycoprotein complex via alpha-syntrophin in glia. *J Biol Chem* 279: 28387–28392, 2004.
7. Connors NC, Kofuji P. Potassium channel Kir4.1 macromolecular complex in retinal glial cells. *Glia* 53: 124–131, 2006.
8. Cox LA, Adrian GS. Posttranscriptional regulation of chimeric human transferrin genes by iron. *Biochemistry* 32: 4738–4745, 1993.
9. Cremers CW, Admiral RJ, Huygen PL, Bolder C, Everett LA, Joosten FB, Green ED, van Camp G, Otten BJ. Progressive hearing loss, hypoplasia of the cochlea and widened vestibular aqueducts are very common features in Pendred's syndrome. *Int J Pediatr Otorhinolaryngol* 45: 113–123, 1998.
10. Crow JP, Spruell C, Chen J, Gunn C, Ischiropoulos H, Tsai M, Smith CD, Radi R, Koppenol WH, Beckman JS. On the pH-dependent yield of hydroxyl radical products from peroxynitrite. *Free Radic Biol Med* 16: 331–338, 1994.
11. Eisenstein RS. Iron regulatory proteins and the molecular control of mammalian iron metabolism. *Annu Rev Nutr* 20: 627–662, 2000.
12. Everett LA, Belyantseva IA, Noben-Trauth K, Cantos R, Chen A, Thakkar SI, Hoogstraten-Miller SL, Kachar B, Wu DK, Green ED. Targeted disruption of mouse Pds provides insight about the inner-ear defects encountered in Pendred syndrome. *Hum Mol Genet* 10: 153–161, 2001.
13. Everett LA, Glaser B, Beck JC, Idol JR, Buchs A, Heyman M, Adawi F, Hazani E, Nassir E, Baxevanis AD, Sheffield VC, Green ED. Pendred syndrome is caused by mutations in a putative sulphate transporter gene (PDS). *Nat Genet* 17: 411–422, 1997.
14. Everett LA, Morsli H, Wu DK, Green ED. Expression pattern of the mouse ortholog of the Pendred's syndrome gene (Pds) suggests a key role for pendrin in the inner ear. *Proc Natl Acad Sci USA* 96: 9727–9732, 1999.
15. Fish WW. Rapid colorimetric micromethod for the quantitation of complexed iron in biological samples. *Methods Enzymol* 158: 357–364, 1988.
16. Fraser GR. Association of congenital deafness with goitre (pendred's syndrome) a study of 207 families. *Ann Hum Genet* 28: 201–249, 1965.
17. Henderson D, Bielefeld EC, Harris KC, Hu BH. The role of oxidative stress in noise-induced hearing loss. *Ear Hear* 27: 1–19, 2006.
18. Hibino H, Higashi-Shingai K, Fujita A, Iwai K, Ishii M, Kurachi Y. Expression of an inwardly rectifying K<sup>+</sup> channel, Kir5.1, in specific types of fibrocytes in the cochlear lateral wall suggests its functional importance in the establishment of endocochlear potential. *Eur J Neurosci* 19: 76–84, 2004.
19. Iandiev I, Tenckhoff S, Pannicke T, Biedermann B, Hollborn M, Wiedemann P, Reichenbach A, Bringmann A. Differential regulation of Kir4.1 and Kir21 expression in the ischemic rat retina. *Neurosci Lett* 396: 97–101, 2006.
20. Jabba SV, Oelke A, Singh R, Maganti RJ, Fleming S, Wall SM, Everett LA, Green ED, Wangemann P. Macrophage invasion contributes to degeneration of stria vascularis in Pendred syndrome mouse model. *BMC Med* 4: 37, 2006.
21. Johnsen T, Larsen C, Friis J, Hougaard-Jensen F. Pendred's syndrome. Acoustic, vestibular and radiological findings in 17 unrelated patients. *J Laryngol Otol* 101: 1187–1192, 1987.
22. Kaiser M, Maletzki I, Hulsman S, Holtmann B, Schulz-Schaeffer W, Kirchoff F, Bahr M, Neusch C. Progressive loss of a glial potassium channel (KCNJ10) in the spinal cord of the SOD1 (G93A) transgenic mouse model of amyotrophic lateral sclerosis. *J Neurochem* 99: 900–912, 2006.
23. Kusakari J, Ise I, Comegys TH, Thalmann I, Thalmann R. Effect of ethacrynic acid, furosemide, and ouabain upon the endolymphatic potential and upon high energy phosphates of the stria vascularis. *Laryngoscope* 88: 12–37, 1978.
24. Lymar SV, Jiang Q, Hurst JK. Mechanism of carbon dioxide-catalyzed oxidation of tyrosine by peroxynitrite. *Biochemistry* 35: 7855–7861, 1996.
25. Marcus DC, Thalmann R, Marcus NY. Respiratory rate and ATP content of stria vascularis of guinea pig in vitro. *Laryngoscope* 88: 1825–1835, 1978.
26. Marcus DC, Wu T, Wangemann P, Kofuji P. KCNJ10 (Kir4.1) potassium channel knockout abolishes endocochlear potential. *Am J Physiol Cell Physiol* 282: C403–C407, 2002.
27. Muijsers RB, van Den WE, Folkerts G, Beukelman CJ, Koster AS, Postma DS, Nijkamp FP. Apocynin inhibits peroxynitrite formation by murine macrophages. *Br J Pharmacol* 130: 932–936, 2000.
28. Nakaya K, Harbidge DG, Wangemann P, Schultz BD, Green ED, Wall SM, Marcus DC. Lack of pendrin. *Am J Physiol Renal Physiol* 292: F1314–F1321, 2007.
29. Pendred V. Deaf-mutism and goitre. *Lancet* 11: 532, 1896.
30. Radi R. Nitric oxide, oxidants, and protein tyrosine nitration. *Proc Natl Acad Sci USA* 101: 4003–4008, 2004.
31. Ramakers C, Ruijter JM, Deprez RH, Moorman AF. Assumption-free analysis of quantitative real-time polymerase chain reaction (PCR) data. *Neurosci Lett* 339: 62–66, 2003.
32. Reardon W, Coffey R, Phelps PD, Luxon LM, Stephens D, Kendall-Taylor P, Britton KE, Grossman A, Trembath R. Pendred syndrome—100 years of underascertainment? *QJM* 90: 443–447, 1997.
33. Rybak LP, Whitworth CA. Ototoxicity: therapeutic opportunities. *Drug Discov Today* 10: 1313–1321, 2005.
34. Sabolic I. Common mechanisms in nephropathy induced by toxic metals. *Nephron Physiol* 104: 107–114, 2006.
35. Sadanaga M, Morimitsu T. Development of endocochlear potential and its negative component in mouse cochlea. *Hear Res* 89: 155–161, 1995.
36. Sargent PJ, Farnaud S, Evans RW. Structure/function overview of proteins involved in iron storage and transport. *Curr Med Chem* 12: 2683–2693, 2005.
37. Scott DA, Wang R, Kreman TM, Sheffield VC, Karniski LP. The Pendred syndrome gene encodes a chloride-iodide transport protein. *Nat Genet* 21: 440–443, 1999.
38. Stadtman ER. Metal ion-catalyzed oxidation of proteins: biochemical mechanism and biological consequences. *Free Radic Biol Med* 9: 315–325, 1990.
39. Stockklauser C, Ludwig J, Ruppertsberg JP, Klocker N. A sequence motif responsible for ER export and surface expression of Kir2.0 inward rectifier K<sup>+</sup> channels. *FEBS Lett* 493: 129–133, 2001.
40. Vesela A, Wilhelm J. The role of carbon dioxide in free radical reactions of the organism. *Physiol Res* 51: 335–339, 2002.
41. Wangemann P. Supporting sensory transduction: cochlear fluid homeostasis and the endocochlear potential. *J Physiol* 576: 11–21, 2006.
42. Wangemann P, Itza EM, Albrecht B, Wu T, Jabba SV, Maganti RJ, Lee JH, Everett LA, Wall SM, Royaux IE, Green ED, Marcus DC. Loss of KCNJ10 protein expression abolishes endocochlear potential and causes deafness in Pendred syndrome mouse model. *BMC Med* 2: 30, 2004.
43. Wangemann P, Liu J, Marcus DC. Ion transport mechanisms responsible for K<sup>+</sup> secretion and the transepithelial voltage across marginal cells of stria vascularis in vitro. *Hear Res* 84: 19–29, 1995.
44. Wangemann P, Nakaya K, Wu T, Maganti RJ, Itza EM, Sanneman JD, Harbidge DG, Billings S, Marcus DC. Loss of cochlear. *Am J Physiol Renal Physiol* 292: F1345–F1353, 2007.
45. Yamasaki M, Komune S, Shimozone M, Matsuda K, Haruta A. Development of monovalent ions in the endolymph in mouse cochlea. *ORL J Otorhinolaryngol Relat Spec* 62: 241–246, 2000.
46. You HJ, Oh DH, Choi CY, Lee DG, Hahn KS, Moon AR, Jeong HG. Protective effect of metallothionein-III on DNA damage in response to reactive oxygen species. *Biochim Biophys Acta* 1573: 33–38, 2002.